DNA 5376Z

# MEASUREMENT OF IN-SITU SHOCK EFFECTS IN CARBONATE ROCKS

J. Vizgirda
T. J. Ahrens
California Institute of Technology
1201 E. California Boulevard
Pasadena, California 91109

LEVEL II

29 February 1980

Interim Report for Period 30 March 1979—29 February 1980

CONTRACT No. DNA 001-79-C-0252

APPROVED FOR PUBLIC RELEASE;
DISTRIBUTION UNLIMITED.



THIS WORK SPONSORED BY THE DEFENSE NUCLEAR AGENCY
UNDER RDT&E RMSS CODE B344079464 Y99QAXSB04922 H2590D.

Prepared for
Director
DEFENSE NUCLEAR AGENCY
Washington, D. C. 20305

Destroy this report when it is no longer needed. Do not return to sender.

PLEASE NOTIFY THE DEFENSE NUCLEAR AGENCY, ATTN: STTI, WASHINGTON, D.C. 20305, IF YOUR ADDRESS IS INCORRECT, IF YOU WISH TO BE DELETED FROM THE DISTRIBUTION LIST, OR IF THE ADDRESSEE IS NO LONGER EMPLOYED BY YOUR ORGANIZATION.

UNCLASSIFIED

SECURITY CLASSIFICATION OF THIS PAGE (When Data Entered)

12 33

19 REPORT DOCUMENTATION PAGE

READ INSTRUCTIONS BEFORE COMPLETING FORM

| | |
|---|---|
| 1. REPORT NUMBER: 18 DNA 5376Z | 2. GOVT ACCESSION NO.: AD-A095389 |
| 3. RECIPIENT'S CATALOG NUMBER: | |
| 4. TITLE (and Subtitle): 6 MEASUREMENT OF IN-SITU SHOCK EFFECTS IN CARBONATE ROCKS | 5. TYPE OF REPORT & PERIOD COVERED: 9 Interim Report. 30 Mar 79—29 Feb 80 |
| | 6. PERFORMING ORG. REPORT NUMBER: |
| 7. AUTHOR(s): 10 J. Vizgirda, T. J. Ahrens | 8. CONTRACT OR GRANT NUMBER(s): 15 DNA 001-79-C-0252 NEW |
| 9. PERFORMING ORGANIZATION NAME AND ADDRESS: California Institute of Technology, 1201 E. California Blvd., Pasadena, California 91109 | 10. PROGRAM ELEMENT, PROJECT, TASK AREA & WORK UNIT NUMBERS: Subtask Y99QAXSB049-22 16 |
| 11. CONTROLLING OFFICE NAME AND ADDRESS: Director, Defense Nuclear Agency, Washington, D. C. 20305 | 11 12. REPORT DATE: 29 Feb 1980; 13. NUMBER OF PAGES: 34 |
| 14. MONITORING AGENCY NAME & ADDRESS (if different from Controlling Office): 17 B049 | 15. SECURITY CLASS (of this report): UNCLASSIFIED; 15a. DECLASSIFICATION/DOWNGRADING SCHEDULE: N/A |

16. DISTRIBUTION STATEMENT (of this Report)

Approved for public release; distribution unlimited. 62704H

17. DISTRIBUTION STATEMENT (of the abstract entered in Block 20, if different from Report)

18 SUPPLEMENTARY NOTES

This work sponsored by the Defense Nuclear Agency under RDT&E RMSS Code B344079464 Y99QAXSB04922 H2590D.

19 KEY WORDS (Continue on reverse side if necessary and identify by block number)

Ground Motion
Cratering Cactus
Nuclear Explosions
Impact

abst

20 ABSTRACT (Continue on reverse side if necessary and identify by block number)

Detailed X-ray analyses of core samples taken directly beneath Cactus crater revealed a consistent transition from high to low Mg calcite, thus indicating retention of pre-impact stratigraphy and providing strong evidence for the absence of a fall-back breccia lens thicker than ~ 1 m. A downward displacement of 4 to 8 m was determined by comparing the level of the high to low Mg transition in cores taken directly beneath and outside the crater. Detailed examination of the outside, i.e. control, core samples from the critical

DD FORM 1 JAN 73 1473 EDITION OF 1 NOV 65 IS OBSOLETE

UNCLASSIFIED

SECURITY CLASSIFICATION OF THIS PAGE (When Data Entered)

071550

071550 gm

20. ABSTRACT (continued)

transition interval, planned for future investigations, should allow better resolution of the amount of downward displacement of the rocks in the floor of Cactus crater as well as lending insight into the mode of in situ deformation beneath the crater.

We have also continued our research on identifying and applying methods of measurement of shock-induced deformation, and relating, via laboratory and field shock loading, observed shock effects to the shock histories of carbonate rocks from explosion and impact craters. During the last 6 months, we have concentrated on developing the method of peak broadening measurements in X-ray diffractometer spectra. A consistent and reproducible increase in peak widths with increasing shock pressure was observed in aragonite shocked in the laboratory and in nuclear and high explosive blasts. The phenomena producing this broadening may include plastic strain and mosaicism, with the latter being the dominant effect; the sensitivity of the method appears limited to materials shocked above ~ 1 GPa. By correlating aragonite peak widths in laboratory shocked coral with coral core samples drilled from directly beneath Cactus crater, a peak pressure of 2 ± 1.5 GPa was inferred for the shallowest Cactus samples. This value compares favorably with the 4.5 ± 0.5 GPa peak pressures deduced from ESR studies on calcite from these samples. Differences in the X-ray patterns have been observed in single crystal aragonite ostensibly shocked to the same pressure by shock pulses of different duration; those samples experiencing long duration (100 μsec) pulses, as in the Miser's Bluff TNT blast, show significantly greater shock effects than laboratory shocked (1 μsec duration pulse) samples. Having established the viability of the X-ray diffractometer and ESR techniques as shock effect detectors in calcite and aragonite, we are also applying these methods to carbonate samples from the Diablo Hawk experiment and from several meteorite impact structures. The preliminary ESR results obtained for samples from Haughton Astrobleme do show spectral features at least qualitatively similar to those found in experimentally shocked carbonates. We are continuing to study the mechanisms of crystal damage in calcite and aragonite resulting from shock pulses of different time scales.

PREFACE

We appreciate the helpful discussions with B. Ristvet (AFWL) and B. Couch (McClellan AFB) concerning this work, and the guidance of H. Lowenstam and P. Duwez (Caltech) in our X-ray investigations.

TABLE OF CONTENTS

LIST OF ILLUSTRATIONS

## I. INTRODUCTION

During the past 6 months, we have obtained results on the high to low magnesium calcite transition in the core from the 18 kT Pacific Test Site nuclear explosion crater, Cactus, which may have significant bearing on the interpretation of crater structure. Specifically, the results indicate retention of pre-impact stratigraphy, the absence of a fallback breccia lens below 11 m (thus limiting the thickness of such a lens, if present, to $\sim$ 1 m), and coherent downward displacement of the rocks underlying Cactus crater by $\sim$ 6 m. These results are discussed in Section II.

We have also continued our efforts to develop techniques which will be able to detect and place quantitative limits on shock metamorphism in carbonates. Having established the viability of the electron spin resonance (ESR) method for low shock pressure level determinations in calcite, we began to investigate the possibility of using X-ray diffractometer peak broadening (Vizgirda and Ahrens, 1977, Vizgirda et al. 1978, Hanss et al. 1978) in quantitative shock deformation analyses of calcite and aragonite. Tentative trends previously reported were substantiated by re-running the samples on X-ray equipment allowing much higher resolution and by refining the measuring and calculational methods. The results are reported in Section III.

Ultimately, we would like to be able to successfully apply our investigative methods to naturally shocked carbonates. We have taken initial steps in this effort with the ESR technique and found qualitatively similar effects in calcite from a $\sim$ 14 m.y. old meteorite impact crater and in experimentally shocked calcite.

In addition to establishing empirical shock pressure versus deformation correlations for carbonate minerals, we have made attempts to understand the deformation mechanisms responsible for the various spectroscopic effects, and to develop a general framework for understanding the response of calcite and aragonite to dynamically induced strains. Initial efforts in this direction have included ESR investigations of single and polycrystalline calcite and X-ray diffractometer scans of aragonite shocked in the laboratory and in a long duration shock pulse TNT blast. On the basis of these preliminary results, it can be concluded that both the nature of the shock pulse and of the carbonate sample (i.e. single or polycrystalline, porous or non-porous) profoundly affect the observable shock deformation.

Finally, we have reached tentative conclusions regarding the range of shock effects that are retained and may be observed in carbonate minerals, and have better defined the limitations of our detection methods. Proposals for future investigations are guided by the recognition of these possibilities and limitations.

## II. HIGH TO LOW MAGNESIUM CALCITE TRANSITION IN CACTUS CRATER SAMPLES WITH IMPLICATIONS FOR CRATER STRUCTURE

X-ray diffractometer spectra of Cactus crater core material obtained at slow scan speeds of 0.25° 2θ per minute allowed resolution of the high and low magnesium calcite peaks in samples from the top five meters of core, and showed that the transition from high to low Mg content was continuous over this interval.

Fig. 1 shows X-ray powder diffractometer spectra of the five topmost samples from the XC-1 core. The peak at 29.8° is the high Mg calcite peak, corresponding to a $MgCO_3$ content of 14.2 ± 0.4 mole %. The 29.5° 2θ peak corresponds to low Mg calcite, with $MgCO_3$ ranging from 1.5 to 3.1 mole %. (Both represent reflection from the (104) face.) $MgCO_3$ contents were determined from an empirical curve (H. Lowenstam, personal communication, 1979). The results also correspond to the curve relating weight % $MgCO_3$ to 2θ values presented in Chave, 1952. Only the low magnesium peak was present in samples deeper than 15.4 m. The peak at 28.4° 2θ is due to the (111) reflection of an internal silicon standard.

The mole percent of high magnesium calcite, as determined from relative peak height measurements, versus depth of sample is plotted in Fig. 2. Each point represents an averaged high Mg calcite value for 3 aliquots. Note the consistent decrease in the amount of high Mg calcite in the top 5 m of XC-1 core. A least squares fit provides the following relationship for XC-1 depth vs. mole % high magnesium calcite:

$$\text{Depth (m)} = 0.05 \times [\%\ \text{hi Mg calcite}] + 15.586 \qquad [1]$$

The correlation coefficient, $r^2$, is 0.97. High Mg calcite contents for XRU-3 samples are also plotted on this graph. Since no XRU-3 samples between 8 and

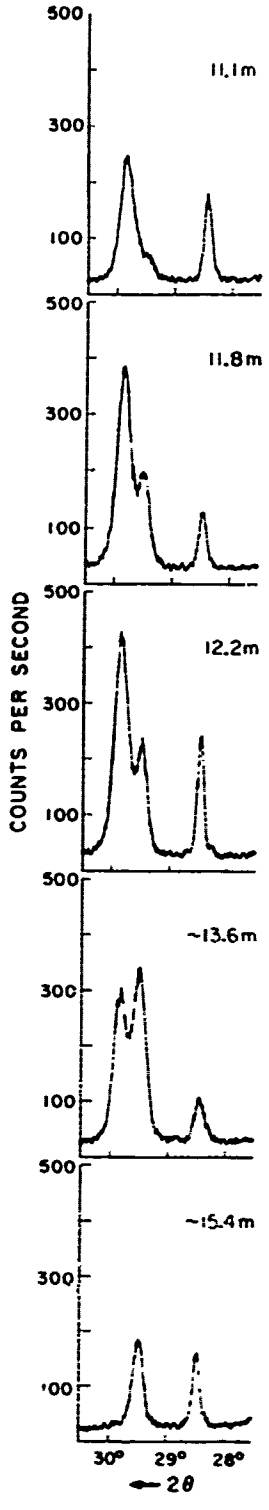


Figure 1: X-ray powder diffractometer spectra of Cactus XC-1 samples; depth are indicated in meters. High magnesium calcite, low magnesium calcite ((104) reflections of both), and silicon standard ((111) reflection) peaks are located at 2θ values of 29.8°,29.5°,and 28.4°, respectively. Note the consistent transition from high to low magnesium calcite from the top of the core to a depth of approximately 15 m.

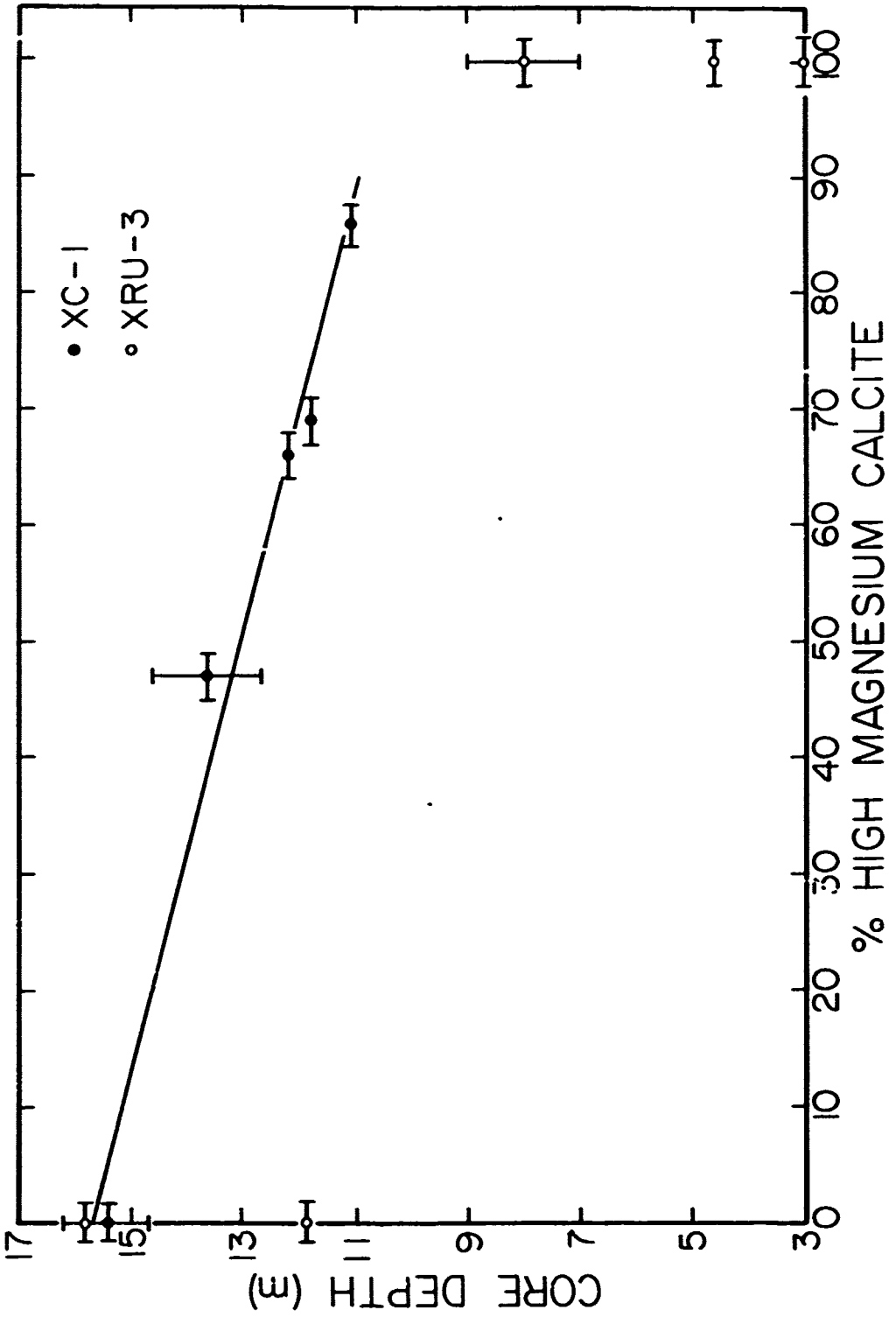


Figure 2: Mole % high magnesium calcite vs. depth in Cactus cores XC-1 and XRU-3. Note the consistent transition, over a 5 m interval, from high to low magnesium calcite in the XC-1 core. A least squares fit provides the following relationship for XC-1 depth vs. % high magnesium calcite: Depth (m) = 0.05 x [% hi Mg calcite] + 15.586.
The correlation coefficient, $r^2$, is 0.97.

12 m were available, it was not possible to trace the Mg content transition in this control core, if, indeed, the transition is present. However, the graph does seem to indicate that the XC-1 core has been depressed 4 to 8 m relative to the XRU-3 core. This relationship, along with the Mg calcite transition in the XC-1 core is depicted in Fig. 3.

The discovery of a gradual transition from high to low Mg calcite in the upper 5 m of Cactus crater core has significant bearing on interpretations of cratering mechanics and simple crater structure. If the trend depicted in Fig. 2 is a representative chemical profile through the upper levels of Cactus crater, then it presents strong evidence for the retention of pre-impact stratigraphy and the absence of a homogeneous fallback breccia lens below 11.1 m, the level of the uppermost XC-1 sample. An allochthonous (i.e. fallback) breccia lens may be present above this level, in which case it has a thickness on the order of 1 m or less. This figure is based on the depth at which the XC-1 core was collared-in and on an estimation of the thickness of sediments accumulated between the time of the nuclear event and the time of drilling by washing in from the crater rim (B. Ristvet, personal communication, 1979). However, below 11 m, the rocks, in all probability, have not been ejected, rather they have been depressed 6 ± 2 m relative to XRU-3 levels.

An alternative interpretation, suggested by B. Ristvet (personal communication, 1979), would explain the X-ray results in terms of a "mixing model". In this model, the starting conditions would be represented by a sharp stratigraphic break between rocks containing only high Mg and only low Mg calcite, occurring below 15 m. During the blast, brecciation and mixing would depress high Mg calcite rock fragments to deeper levels and bring low Mg calcite rocks to shallower levels, thus obliterating the original chemical discontinuity and producing the gradation in Mg calcite depicted in Figs. 2 and 3.

An investigation of XRU-3 samples from the critical levels between 8 and 12 m would, hopefully, provide the evidence needed to support one or the other of the proposed models. In addition, it would allow a better estimate of the amount of depression beneath Cactus crater.

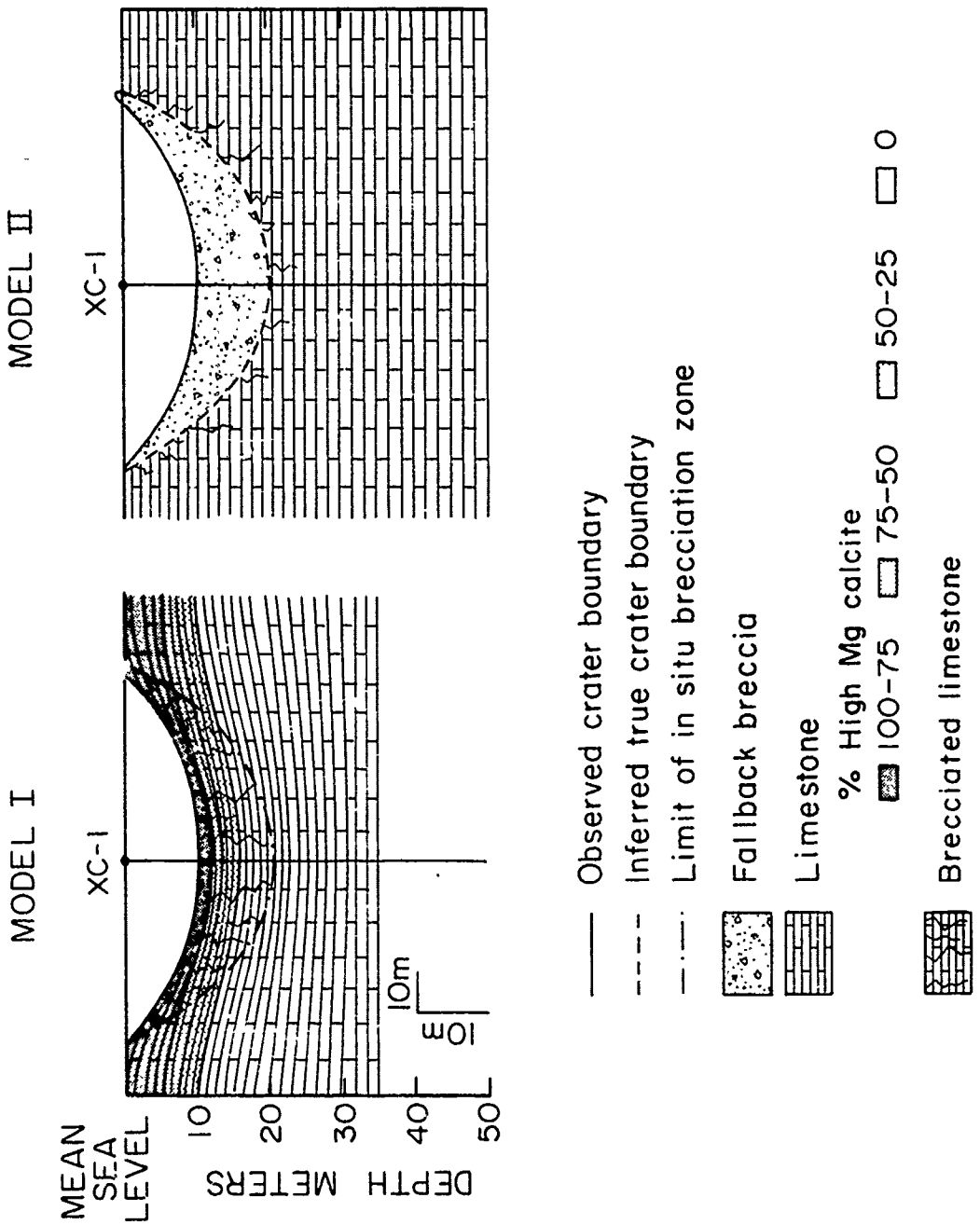


Figure 3: Cross section through Cactus crater showing high to low Mg calcite transition in XC-1 and XRU-3 cores. Details of the transition are not known for the XRU-3 core due to lack of samples between 8 and 12 m. From the information available, a minimum 4 m downward displacement of the rocks underneath Cactus is speculated. Note vertical exaggeration. Viewed looking northeast. (Adapted from Fig. 5.35 of Ristvet et al. 1978)

## III. SHOCK-INDUCED MOSAICISM OF ARAGONITE CRYSTALS

Previously, we had reported preliminary results showing X-ray diffraction peak broadening in samples from the upper levels of the XC-1 Cactus crater core. In the past six months, we have re-analyzed these samples, together with experimentally shock-loaded coral and single crystal aragonite; the results confirm our original observation of diffraction peak broadening in shocked carbonate samples.

The description of the X-ray analyses and measurement techniques is presented in the Appendix. Crystallite sizes were determined using measured peak widths at half-heights, corrected for instrumental broadening. Aragonite rather than calcite was chosen for the investigation of peak broadening in Cactus samples in order to minimize possible interference from compositional variations; the $MgCO_3$ content of calcite, as described in the previous section, is variable in the range of 1.5 to $\sim$ 14 mole %, whereas aragonite is relatively pure and tends to conform to the ideal formula (Deer, Howie and Zussman, 1966). Widths of aragonite peaks at 26.2° and 27.2° 2θ, corresponding to reflections from (11$\bar{1}$) and (021) respectively, were both measured and used to compute crystallite sizes. There was no consistent variation between the two sets of values and the results agreed to within 500 Å. The crystallite sizes plotted in Fig. 4 represent an average of 26.2° and 27.2° 2θ peak widths for at least two sample preparations. Generally, enough material for only one X-ray sample preparation was retrieved in a shock recovery experiment. In such cases, the sample was re-dispersed and a second X-ray diffraction spectrum was made; averaged results from these two scans are plotted in Figs. 5 and 6.

Crystallite sizes were calculated from peak widths using the Scherrer formula (Cullity, 1956).

$$t = \frac{0.9\ \lambda}{\beta \sin \Theta} \qquad [2]$$

where $t$ = crystallite thickness (Å)

$\lambda$ = wavelength of radiation used (Å)

$\beta$ = peak width at half height in terms of 2θ (radians)

$\Theta$ = diffracting angle

Crystallite thickness refers not to sample particle size, but to the average dimension of the effective coherently diffracting domain. The peak width, $\beta$, refers to the measured width minus the broadening due to instrumental effects.

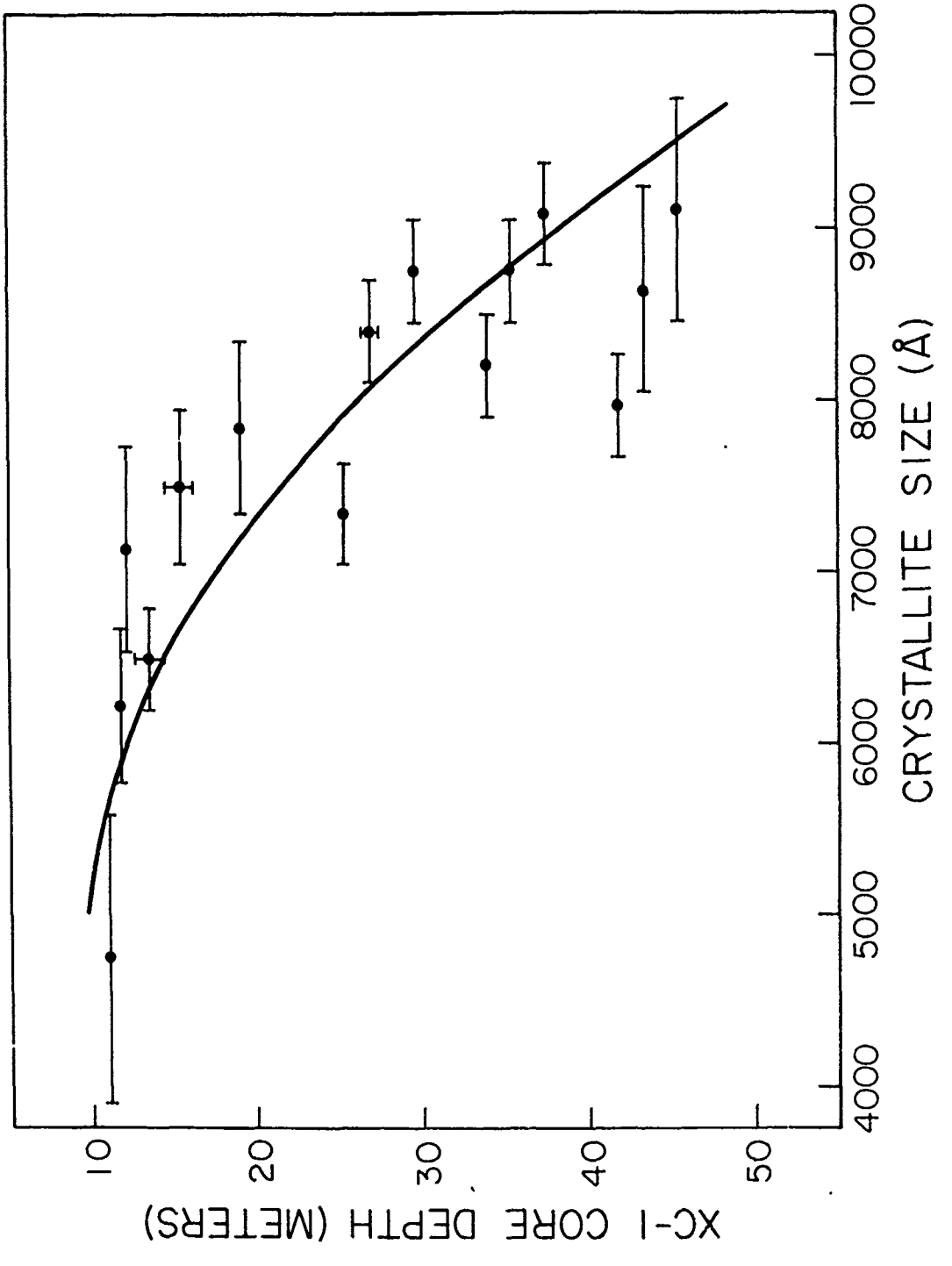


Figure 4: Decrease of effective diffracting aragonite crystallite size (thickness) with decreasing depth in the Cactus XC-1 core. The equation for the exponential curve fit is:

Depth (m) = 1.16 exp [0.0004 x size (Å)]

$r^2 = 0.76$

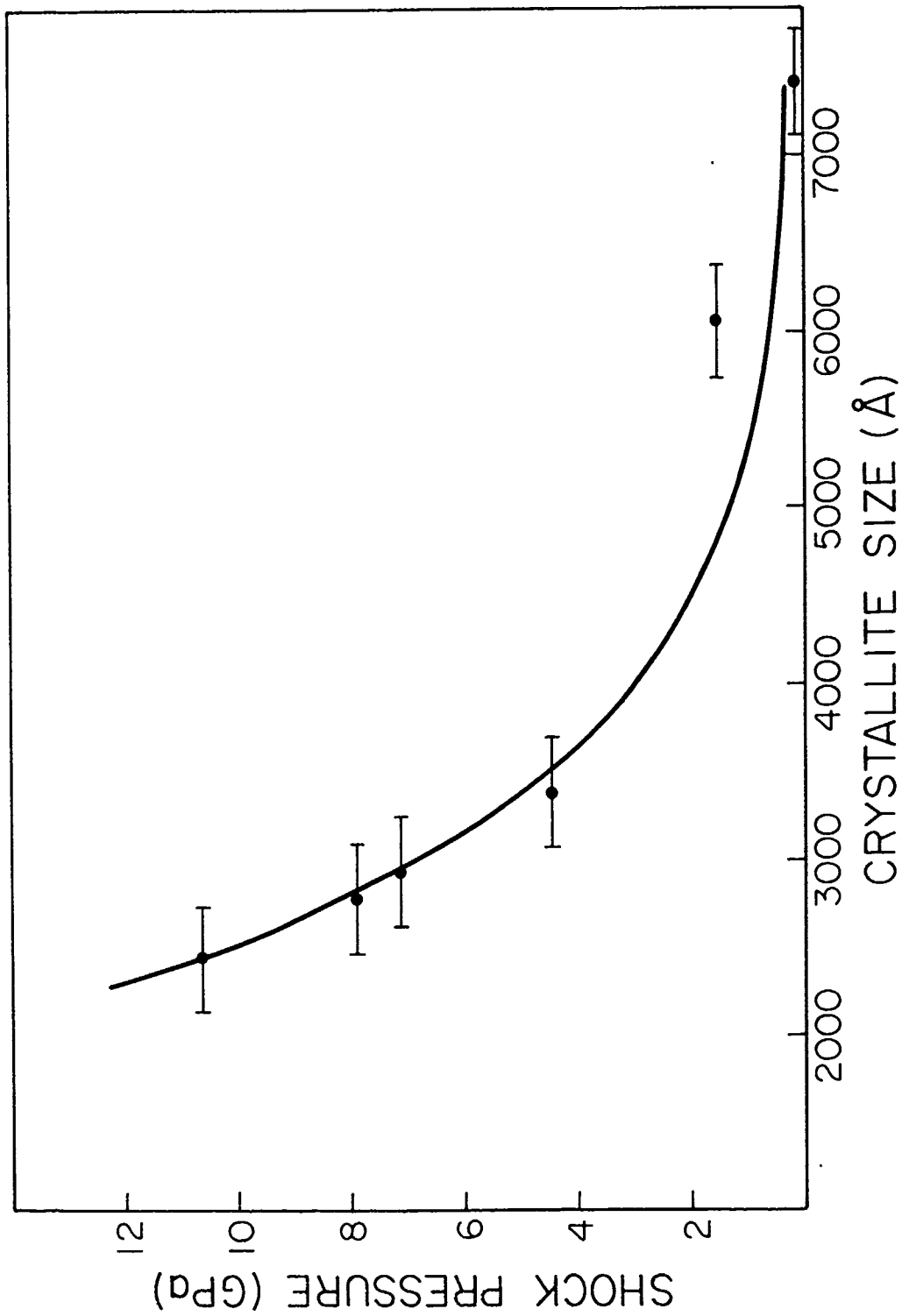


Figure 5: Aragonite crystallite size decrease with increasing shock pressure. The exponential curve fit is:

$$\text{Pressure (GPa)} = 80.71 \exp [-0.0008 \times \text{size (Å)}]$$

$$r^2 = 0.85$$

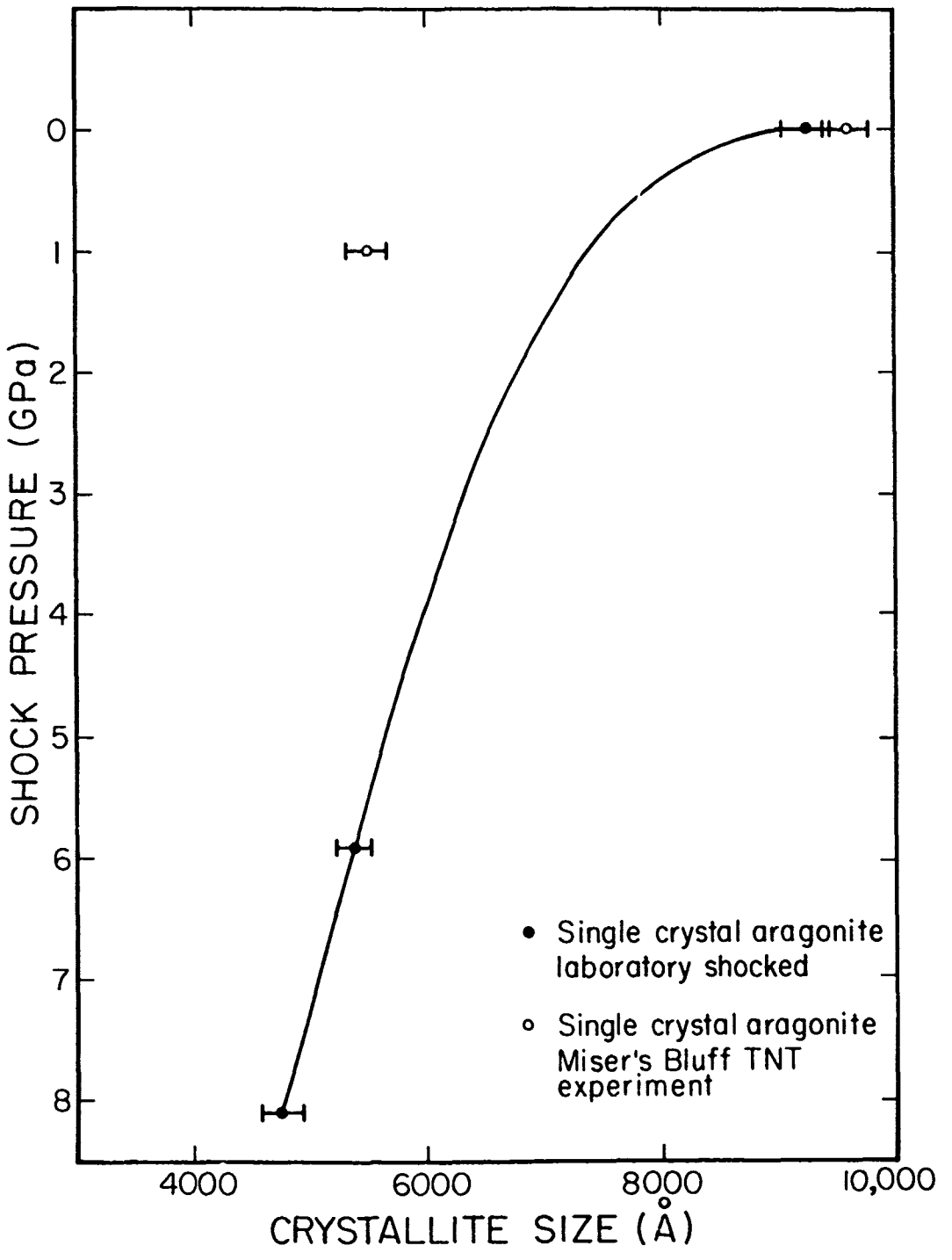


Figure 6: Crystallite size decrease in experimentally shocked single crystal aragonite. Solid circles represent laboratory shocked specimens; the time between onset of the shock and rarefaction waves in these experiments was on the order of 1 microsecond. Open circles represent crystals shocked in the Miser's Bluff TNT experiment, where the time scale was on the order of 100 microseconds. The exponential curve fit to the laboratory shocked aragonite is:

$$\text{Pressure (GPa)} = 5.6 \times 10^{14} \exp\,[-0.006 \times \text{size (Å)}]$$

with a correlation coefficient, $r^2$, of 0.99.

In our analysis we have contributed the observed broadening to the crystallite size effect entirely. However, other factors, such as lattice spacing variations and plastic strain, may contribute to peak broadening as well. As discussed in Section V, Guinier investigations of carbonates, both calcite and aragonite, shocked to pressures below 10 GPa, have not yielded definitive results on lattice parameter changes. In any event, we suspect the lattice parameter shifts in Cactus calcite, should they occur, to be on the order of thousandths of angstroms (Vizgirda et al., submitted for publication, 1979); similar changes present in aragonite minerals from Cactus samples would not be detectable with the X-ray diffractometer. In X-ray investigations of shock-impacted silicate minerals (Hörz and Quaide, 1973; Hanss et al. 1978), it has been assumed that mosaicism dominates over plastic deformation. We have not discounted a contribution from strain to peak broadening, but are unable, from data presently available, to quantify these effects; therefore, in our calculations, all the peak broadening was attributed to mosaicism. The contention that strain effects are quantitatively subordinate to mosaicism is supported by the "reasonable" crystallite sizes calculated for our samples (larger than for deformed metals, but proportionately so to the increased carbonate cell size).

Calculated aragonite crystallite sizes for XC-1 samples are listed in Table 1, and plotted in Fig. 4. A decrease in crystallite size with depth (hence shock pressure) is most pronounced for the upper 15 m of XC-1 core. Below this level, there is a suggestion of continuously increasing crystallite sizes with depth; however, the wide scatter of data and large error bars preclude definition of such a trend. ESR results on calcite from Cactus samples led to similar conclusions. The exponential curve fit to the line is:

$$\text{Depth (m)} = 1.16 \exp [0.0004 \times \text{size (Å)}] \qquad [3]$$

The correlation coefficient, $r^2$, is 0.76.

Data for experimentally shocked coral are listed in Table II and plotted in Fig. 5. The exponential curve fit is:

$$\text{Pressure (GPa)} = 80.71 \exp [-0.0008 \times \text{size (Å)}] \qquad [4]$$

$r^2$ is 0.85.

TABLE I

CACTUS CORE XC-1 SAMPLES -

DEPTH VS. ARAGONITE CRYSTALLITE SIZE

| Depth (meters) | Crystallite Size (Å) |
|---|---|
| 11.1 | 4750 ± 850 |
| 11.8 | 6218 ± 450 |
| 12.2 | 7134 ± 600 |
| 12.7-14.6 | 6504 ± 300 |
| 14.6-16.2 | 7505 ± 450 |
| 19.2 | 7848 ± 500 |
| 25.4 | 7332 ± 300 |
| 26.5-27.7 | 8400 ± 300 |
| 29.7 | 8766 ± 300 |
| 34.1 | 8210 ± 300 |
| 35.4 | 8766 ± 300 |
| 37.5 | 9077 ± 300 |
| 40.8 | |
| 41.8 | 7969 ± 300 |
| 43.3 | 8637 ± 600 |
| 45.4 | 9099 ± 650 |

TABLE II

EXPERIMENTALLY SHOCKED CORAL

PRESSURE VS. ARAGONITE CRYSTALLITE SIZE

| Pressure (GPa) | Crystallite Size (Å) |
|---|---|
| 0.15 | 7485 ± 300 |
| 1.54 | 6051 ± 300 |
| 4.42 | 3376 ± 300 |
| 7.14 | 2928 ± 300 |
| 7.90 | 2785 ± 300 |
| 10.62 | 2437 ± 300 |

Comparing Figs. 4 and 5, a pressure of $\sim$ 2 GPa would correspond to the topmost XC-1 sample. This value is of the same order of magnitude as the 4.5 ± 0.5 GPa peak pressure determined from ESR studies of XC-1 calcite (Vizgirda et al. 1979). The agreement between these two values is encouraging, particularly considering the fact that they were obtained using two different techniques which measured varying modes of shock deformation on two different minerals. Note, also, that the lower size limit for the 11.1 m sample corresponds to a shock pressure of $\sim$ 3.5 GPa, which is very similar to the ESR results.

Fig. 6 compares X-ray results from laboratory shocked single crystal aragonite to that shocked in the Miser's Bluff TNT experiment. It appears from the results plotted that the longer shock pulse (on the order of 100 microseconds) in the TNT blast resulted in a significantly greater amount of damage, i.e. mosaicism than the laboratory produced shock (on the order of 1 microsecond). The exponential curve fit to the laboratory shocked aragonite is:

$$\text{Pressure (GPa)} = 5.6 \times 10^{14} \exp [0.006 \times \text{size } (\mathring{A})] \qquad [5]$$

$r^2 = 0.99$. ESR results on calcite from the Miser's Bluff experiments do not, however, confirm these findings. The varying responses of calcite and aragonite to short and long duration shock pulses require further investigation before such comparisons can be made.

## IV. ELECTRON SPIN RESONANCE INVESTIGATIONS

In the past 6 months, we have completed our ESR investigation of the Cactus crater samples and have submitted the results for publication to Geochimica Cosmochimica Acta.

ESR investigations of experimentally shocked single and polycrystalline calcite have also been conducted. Unlike the Cactus coral samples, the experimentally shocked calcites do not show a measurable decrease in the amount of $Mn^{2+}$ hyperfine peak splitting. (The polycrystalline samples may show a slight decrease; however, considering the measurement errors and the fact that only two shocked samples are available, no definitive statements can be made.) Qualitative spectral changes in shocked samples are, however, similar to those observed in the Cactus coral samples. The double character of the central spin transition peaks (see Fig. 7) is observed to become less pronounced,

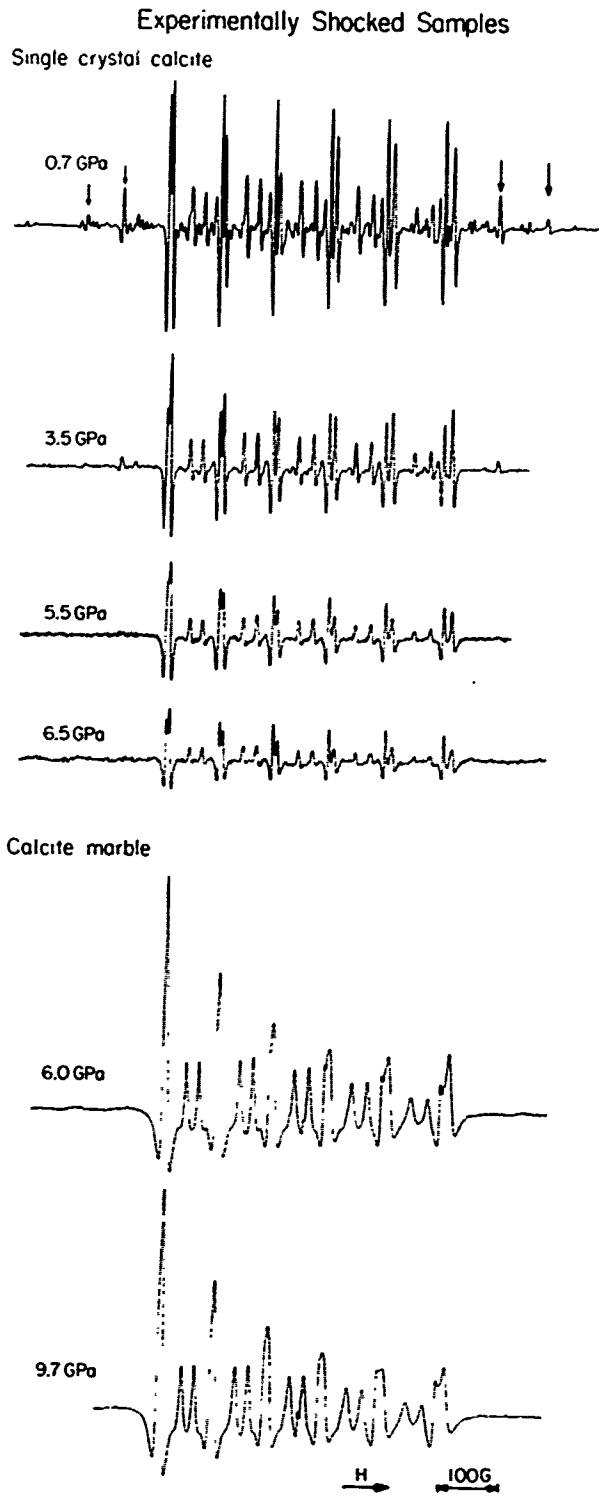


Figure 7: Second derivative electron spin resonance spectra, taken at X-band frequency, of experimentally shocked single and polycrystalline calcite samples showing $Mn^{2+}$ absorption peak variations with shock pressure. The six prominent peaks in the center of the spectra are due to the central $Mn^{2+}$ spin transitions, $M_S = +1/2 \leftrightarrow -1/2$, $\Delta m_I = 0$. Non-central spin transitions are indicated by arrows.

and, in the low field peaks (i.e. in the direction of decreasing magnetic field, H) to eventually disappear, with increasing shock pressure. Also, absorption peaks due to non-central spin transitions (arrows in the figure) are seen to disappear at higher shock pressures. (For a detailed discussion of the $Mn^{2+}$ ESR spectrum in calcite, refer to the included manuscript.) Note also, the differences in the spectra of single crystal calcite shocked to 6.5 GPa and marble shocked to 6.0 GPa; from these preliminary results, it may be concluded that polycrystalline samples show greater degrees of shock damage than single crystal samples shocked to approximately the same levels. It may also be speculated that porous, water-saturated, multi-phase material, such as the Cactus coral samples, would show even greater degrees of shock deformation.

Fig. 8 presents spectra of samples from the Haughton Astrobleme in the Canadian Arctic. The first spectrum is that of a dark-grey clast which, in hand specimen, appears to be unshocked. The second spectrum is that of alight grey, highly sheared clast. The third is that of the finely comminuted matrix of the impact breccia. Both the second and third spectra show absorption peak changes characteristic of the experimentally shocked calcite (See Fig. 7) that is, fading of the double peak character at the low field end of the spectrum, and diminution and final disappearance of the non-central spin transition peaks. Comparing the Haughton and experimentally shocked samples yields preliminary shock pressure levels of 4 GPa ± 2 GPa and 6 HPa ± 2 GPa for the sheared clast and matrix samples respectively.

## V. INVESTIGATION OF SHOCK-INDUCED LATTICE PARAMETER CHANGES

An attempt was made to detect and quantify lattice parameter changes suggested by ESR results on calcite from Cactus crater. X-ray data was obtained on a Guinier camera using $CuK\alpha_1$ radiation; a least squares refinement of the data yielded cell parameters.

Due to the variability in chemistry of calcite from Cactus crater, lattice parameter changes in the mineral could not be determined with the Guinier method. However, the aragonite in these samples showed relatively well-defined lines, but no measurable shift was observed. Laboratory shocked single crystal calcite (to 6.5 GPa) and aragonite (to 8.1 GPa) showed lines that were increasingly diffuse at higher pressures, but there was no measurable shift in position. (A slight shift, corresponding to, say, $\sim$ 0.005 Å, would

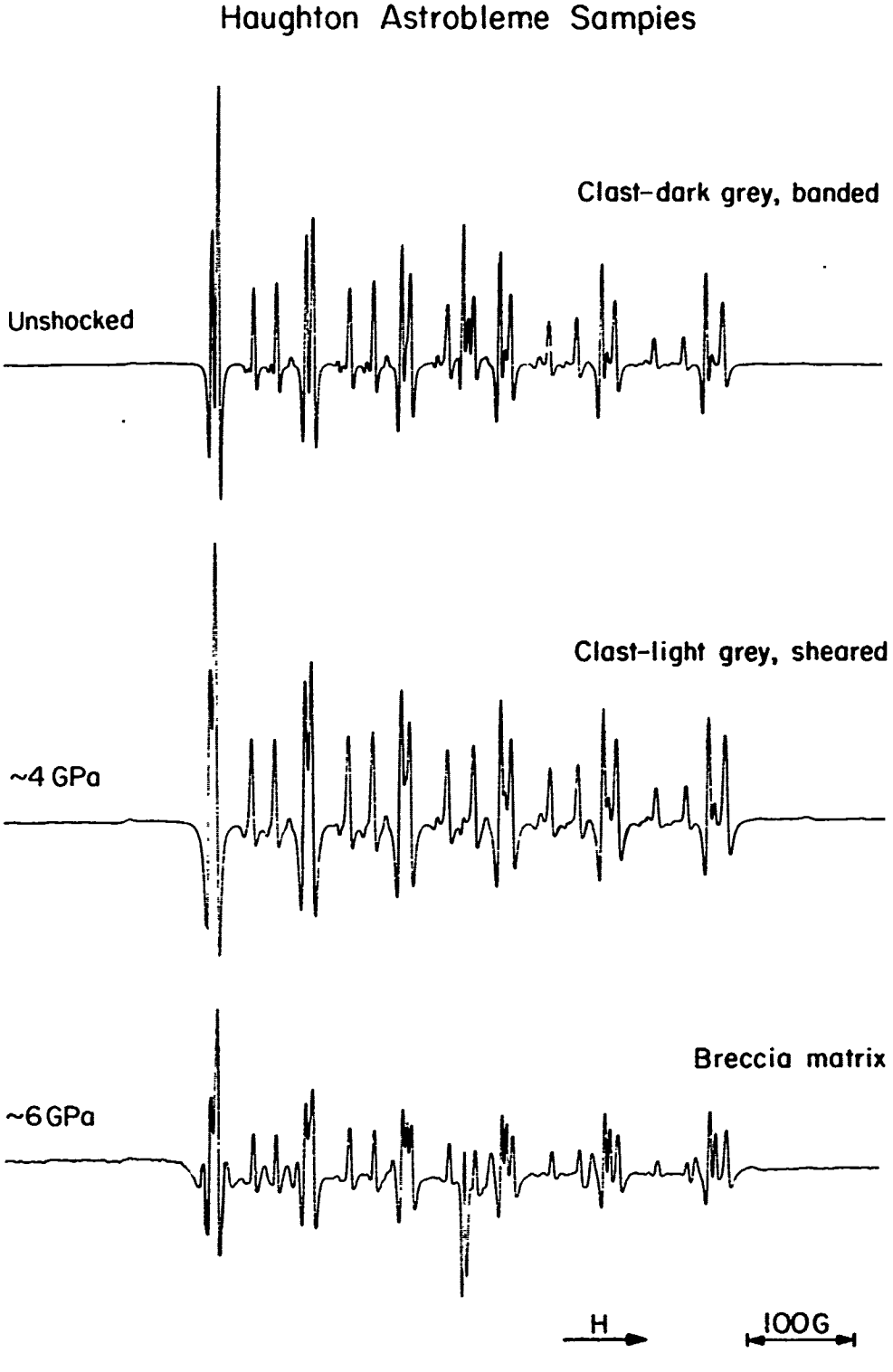


Figure 8: Second derivative electron spin resonance absorption spectra demonstrating the loss of fine structure of $Mn^{2+}$ resonance in limestone from the fallback breccia unit at Haughton crater.

have been extremely difficult to detect due to extreme line broadening.)

The Miser's Bluff calcite samples provided the most accurate, and most reproducible data. The results are plotted in Fig. 9. An increase in lattice parameter is observed in calcite purportedly shocked to 1.0 and 0.1 GPa; note that the magnitude of the increase is $\lesssim$ 0.01 Å. The other samples remain in the range of unshocked calcite. The discrepancies in the data may be due to 1) inaccurate pressure gauge values, 2) local pressure variations due to inhomogeneities in the detonation medium (alluvium) inducing stresses in the samples which do not correspond with gauge readings, or 3) insufficient resolution provided by the Guinier technique. We suggest all 3 factors to be responsible. Aragonite from the Miser's Bluff experiment did not show any measurable increase in cell dimensions.

In general, the results from our Guinier investigations have proved inconclusive. The fact that no definitive trends in lattice parameter shifts in shocked calcite and aragonite were observed may be due to the large margin for error in the method used, and not the lack of such trends. In any event, no further Guinier investigations are planned.

## VI. CONCLUSIONS

Based on the results presented in this report, the following conclusions and recommendations for continued investigations are made:

1) The gradual transition from high to low magnesium calcite, observed below the 11.1 m level in the Cactus XC-1 core, indicates retention of pre-impact stratigraphy and lack of a fallback breccia lens thicker than $\sim$ 1 m. Comparing the level of the transition to that observed in the XRU-3 core, it appears that rocks beneath Cactus crater have been depressed 4 to 8 m. It would be of great interest to obtain and analyze samples from the 8 to 12 m levels in the XRU-3 core. Results from these samples would resolve the position and nature of the high to low Mg calcite transition outside the crater, thereby allowing determination of the amount of downward displacement and lending insight into the mode of in situ deformation beneath Cactus crater. The existence of stratigraphic control on such a fine scale provides a unique opportunity to study structural characteristics of simple craters.

2) Peak broadening in X-ray diffractometer spectra has been observed in aragonite minerals shock-loaded in the laboratory and in nuclear and high-

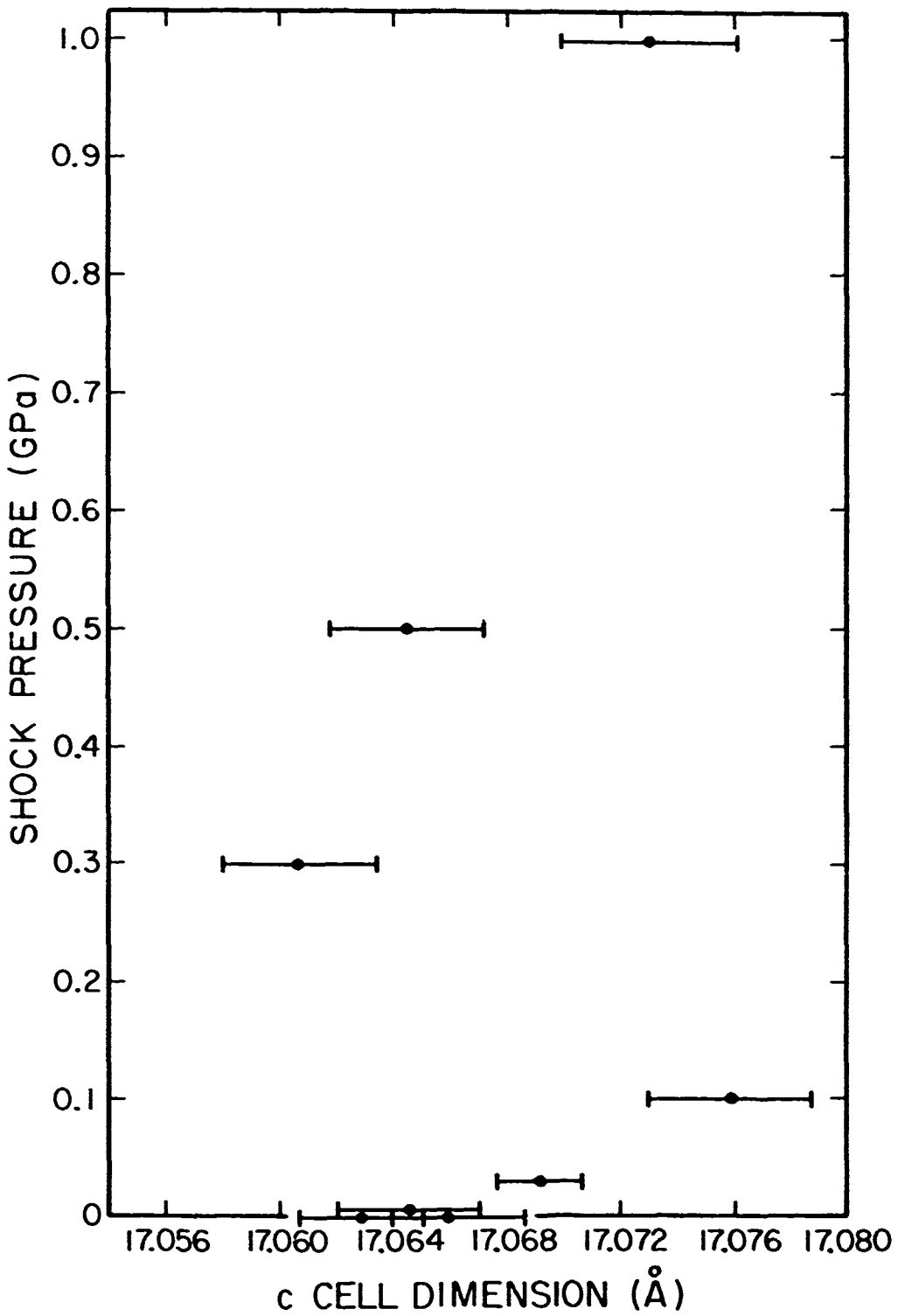


Figure 9: Lattice parameter (c dimension) variation with shock pressure in single crystal calcite shock loaded in the Miser's Bluff TNT experiment.

explosive blasts. The increase in peak width with increasing shock pressure has proven to be a consistent and reproducible effect sensitive to shock pressures $\gtrsim$ 1 GPa. What remains to be investigated is the cause (or causes) of this broadening; mosaicism and plastic strain effects may both be responsible. The degree to which these mechanisms act in carbonate mineral deformation will require further refinement of the X-ray diffractometer data and comparison with single crystal X-ray results. Annealing studies (to investigate the possibility of plastic strain) are also planned.

Peak pressures determined for Cactus core samples ($\sim$ 2 GPa) with the X-ray method are of the same order of magnitude as those obtained from ESR investigations, although they may be lower by a factor of $\sim$ 2. Several issues need to be considered before pressures obtained from X-ray and ESR methods can be compared. These include the varying responses of the two different minerals tested, calcite and aragonite, to long and short duration pulses, and to the different modes of deformation being detected by the two methods used. In an attempt to resolve these issues we intend to analyze single and polycrystalline calcite samples of constant composition, experimentally shocked with both long (Miser's Bluff and Diablo Hawk blasts) and short (laboratory experiments) duration pulses, using the X-ray peak broadening technique.

## REFERENCES


Chave, K. E. (1952): A solid solution between calcite and dolomite. J. Geology, 60, 190-192.

Cullity, B. D. (1956): Elements of X-Ray Diffraction. Addison-Wesley Publishing Company, Inc., Reading, Mass., 96-99.

Deer, W. A., Howie, R. A., and Zussman, J. (1966): An Introduction to the Rock-Forming Minerals. Longman, London, 497-501.

Hanss, R. E., Montague, B. R., Davis, M. K., and Galindo, C. (1978): X-ray diffractometer studies of shocked materials. Proc. Lunar Planet. Sci. Conf. 9th, 2773-2787.

Hörz, F. and Quaide, W. L. (1973): Debye-Scherrer investigations of experimentally shocked silicates. The Moon, 6, 45-82.

Ristvet, B. L., Tremba, E. L., Couch, R. F., Fetzer, J. A., Goter, E. R., Walter, D. R., and Wendland, V. P. (1978): Geologic and geophysical investigations of the Eniwetok nuclear craters. Air Force Weapons Laboratory, Final Report.

Vizgirda, J. and Ahrens, T. J. (1977): Shock effects in carbonate rocks. Interim Final Report to DNA, Dec. 1, 1977.

Vizgirda, J., Ahrens, T. J., and Tsay, F. (1978): X-ray diffraction and ESR studies of shocked calcium carbonate (abstract). Bull. Am. Physical Society, 23, no. 1, Jan. 1978, p. 105.

Vizgirda, J., Ahrens, T. J., and Tsay, F. (1979): Shock-induced effects in calcite from Cactus crater. submitted for publication to Geochim. Cosmochim. Acta, Oct. 1979.

# APPENDIX

## X-RAY DIFFRACTION EXPERIMENTAL PROCEDURE

X-ray powder diffractometer scans were obtained on a Norelco type 12045 B-3 unit operating at 45kv, 20 ma, and using nickel filtered copper Kα radiation. Voltage and amperage settings, as well as the time constant, range (500 counts per second), and slit configuration, were kept constant for the series of experiments. A slow scan speed of 0.25° 2θ per minute allowed resolution of the high and low magnesium calcite peaks and accurate determinations of peak widths.

Coral core and single and polycrystalline carbonate samples were ground, in alcohol, in an agate mortar until powdered. The effect of grinding on the X-ray results (specifically, on the peak broadening measurements) was investigated by comparing spectra of several aliquots of a particular coral sample, one of which was not ground at all, and two others requiring different amounts of grinding; there was no measurable difference in broadening between the three samples. The powder was then sieved to pass through a 325, but not a 400 mesh cloth, i.e., a standard size fraction between 38 and 43 microns was obtained. The sieving procedure did not appear to preferentially concentrate any phases, since spectra taken before and after show the same calcite to aragonite ratios. Sample powders were then mixed with approximately 8 mg of Si standard powder, wetted with methanol, and compacted into Lexan sample holder wells with an approximate capacity of 0.07 cc.

In order to determine crystallite sizes from diffraction peak profiles, measured line breadths were corrected for instrumental broadening. Precisely cut single crystals of quartz (10$\bar{1}$1 face) and MgO (001 face) were used to determine the instrumental peak width of 0.12° 2θ.

Peak heights and widths were measured using a magnifying scale. Since the background signal proved to be reproducible, an overlay with this signal and a drawn baseline was used to determine peak heights. With this method, measurements of peak widths at half heights could be duplicated to within 0.004° 2θ, resulting in a 2% error in calculated crystallite sizes.

# DISTRIBUTION LIST

DEPARTMENT OF DEFENSE

Assistant to the Secretary of Defense
Atomic Energy
ATTN: Executive Assistant

Defense Advanced Rsch Proj Agency
ATTN: TIO
ATTN: G. Bulin

Defense Intelligence Agency
ATTN: DB-4C, E. O'Farrell
ATTN: DB-4N

Defense Nuclear Agency
2 cy ATTN: SPSS
4 cy ATTN: TITL

Defense Technical Information Center
12 cy ATTN: DD

Field Command
Defense Nuclear Agency
ATTN: FCPR
ATTN: FCTMOF

Field Command
Defense Nuclear Agency
Livermore Division
ATTN: FCPRL

Interservice Nuclear Weapons School
ATTN: TTV

Joint Strat Tgt Planning Staff
ATTN: JLA
ATTN: NRI-STINFO Library

NATO School (SHAPE)
ATTN: U.S. Documents Officer

Undersecretary of Def for Rsch & Engrg
Department of Defense
ATTN: Strategic & Space Systems (OS)

DEPARTMENT OF THE ARMY

BMD Advanced Technology Center
Department of the Army
ATTN: 1CRDABH-X
ATTN: ATC-T

Chief of Engineers
Department of the Army
ATTN: DAEN-RDM
ATTN: DAEN-MCE-D

Harry Diamond Laboratories
Department of the Army
ATTN: DELHD-I-TL
ATTN: DELHD-N-P

U.S. Army Ballistic Research Labs
ATTN: DRDAR-BLV
ATTN: DRDAR-TSB-S
ATTN: DRDAR-BLE, J. Keefer

DEPARTMENT OF THE ARMY (Continued)

U.S. Army Concepts Analysis Agency
ATTN: CSSA/ADL

U.S. Army Engineer Center
ATTN: DT-LRC

U.S. Army Engineer Div Huntsville
ATTN: HNDED-SR

U.S. Army Engineer Div Ohio River
ATTN: ORDAS-L

U.S. Army Eng Waterways Exper Station
ATTN: WESSD, J. Jackson
ATTN: WESSA, W. Flathau
ATTN: J. Zelasko
ATTN: WESSE, L. Ingram
ATTN: Library
ATTN: J. Drake
ATTN: J. Strange

U.S. Army Material & Mechanics Rsch Ctr
ATTN: Technical Library

U.S. Army Materiel Dev & Readiness Cmd
ATTN: DRXAM-TL

U.S. Army Missile Command
ATTN: RSIC

U.S. Army Nuclear & Chemical Agency
ATTN: Library

DEPARTMENT OF THE NAVY

Naval Construction Battalion Cntr
Civil Engineering Laboratory
ATTN: Code L08A
ATTN: Code L51, R. O'Dello
ATTN: Code L51, S. Takahashi

Naval Electronic Systems Command
ATTN: PME 117-21

Naval Facilities Engineering Command
ATTN: Code 04B
ATTN: Code 03T
ATTN: Code 09M22C

Naval Material Command
ATTN: MAT 08T-22

Naval Postgraduate School
ATTN: Code 0142 Library
ATTN: G. Lindsay

Naval Research Laboratory
ATTN: Code 2627

Naval Surface Weapons Center
ATTN: Code F31

Naval Surface Weapons Center
ATTN: Tech Library & Info Services Branch

DEPARTMENT OF THE NAVY (Continued)

Naval War College
ATTN: Code E-11

Naval Weapons Evaluation Facility
ATTN: Code 10

Newport Laboratory
Naval Underwater Systems Center
ATTN: Code EM, J. Kalinowski

Office of Naval Research
ATTN: Code 715
ATTN: Code 474, N. Perrone

Office of the Chief of Naval Operations
ATTN: OP 981
ATTN: OP 03EG

Strategic Systems Project Office
Department of the Navy
ATTN: NSP-43

DEPARTMENT OF THE AIR FORCE

Air Force Geophysics Laboratory
ATTN: LWW. K. Thompson

Air Force Institute of Technology
ATTN: Library

Air Force Office of Scientific Research
ATTN: J. Allenn
ATTN: W. Best

Air Force Systems Command
ATTN: DLW

Air Force Weapons Laboratory
Air Force Systems Command
ATTN: NTE, M. Plamondon
ATTN: NTES, R. Jolley
ATTN: NTES, J. Thomas
ATTN: NTES-C, R. Henny
ATTN: SUL

Assistant Chief of Staff
Intelligence
Department of the Air Force
ATTN: INT

Ballistic Missile Office
Air Force Systems Command
ATTN: MNNXH, D. Gage
ATTN: MNNH, M. Delvecchio
ATTN: MNN

Deputy Chief of Staff
Research, Development & Acq
Department of the Air Force
ATTN: AFRDQSM

Deputy Chief of Staff
Logistics & Engineering
Department of the Air Force
ATTN: LEEE

Foreign Technology Division
Air Force Systems Command
ATTN: NIIS Library

DEPARTMENT OF THE AIR FORCE (Continued)

Rome Air Development Center
Air Force Systems Command
ATTN: TSLD

Strategic Air Command/XPFS
Department of the Air Force
ATTN: NRI-STINFO Library

VELA Seismology Center
ATTN: G. Ullrich

DEPARTMENT OF ENERGY

Department of Energy
Albuquerque Operations Office
ATTN: CTID

DEPARTMENT OF ENERGY CONTRACTORS

Nevada Operations Office
Department of Energy
ATTN: Mail & Records for Tech Library

Lawrence Livermore National Laboratory
ATTN: Tech Info Dept Library
ATTN: D. Glenn

Los Alamos National Scientific Lab
ATTN: MS 364
ATTN: R. Bridwell
ATTN: MS 670, J. Hopkins

Sandia National Labs
Livermore Laboratory
ATTN: Library & Security Class Div

Sandia National Labs
ATTN: L. Hill
ATTN: 3141
ATTN: A. Chabai

Oak Ridge National Laboratory
Nuclear Division
ATTN: Central Research Library
ATTN: Civil Def Res Proj

OTHER GOVERNMENT AGENCIES

Central Intelligence Agency
ATTN: OSWR/NED

Department of the Interior
Bureau of Mines
ATTN: Tech Lib

Federal Emergency Management Agency
ATTN: Hazard Eval & Vul Red Div

DEPARTMENT OF DEFENSE CONTRACTORS

Aerospace Corp
ATTN: Tech Info Services

Agbabian Associates
ATTN: M. Agbabian

Applied Theory, Inc
2 cy ATTN: J. Trulio

DEPARTMENT OF DEFENSE CONTRACTORS (Continued)

BDM Corp
ATTN: Corporate Library
ATTN: T. Neighbors

California Institute of Technology
ATTN: T. Ahrens

California Research & Technology, Inc
ATTN: M. Rosenblatt
ATTN: Library
ATTN: S. Schuster
ATTN: K. Kreyenhagen

California Research & Technology, Inc
ATTN: D. Orphal

Calspan Corp
ATTN: Library

University of Denver
Denver Research Institute
ATTN: Sec Officer for J. Wisotski

EG&G Washington Analytical Services Center, Inc
ATTN: Library

Eric H. Wang
Civil Engineering Rsch Fac
University of New Mexico
ATTN: N. Baum

GARD, Inc
ATTN: G. Neidhardt

General Electric Company—TEMPO
ATTN: DASIAC

Applied Rsch Assoc, Inc
ATTN: H. Auld
ATTN: N. Higgins
ATTN: J. Bratton

Higgins, Auld & Associates, Inc
ATTN: S. Blouin

IIT Research Institute
ATTN: M. Johnson
ATTN: R. Welch
ATTN: Documents Library

Institute for Defense Analyses
ATTN: Classified Library

J. H. Wiggins, Inc
ATTN: J. Collins

Kaman AviDyne
ATTN: N. Hobbs
ATTN: Library

Kaman Sciences Corp
ATTN: Library

Lockheed Missiles & Space Co, Inc
ATTN: T. Geers
ATTN: Technical Information Center

Lovelace Biomed & Enviro Rsch Inst, Inc
ATTN: R. Jones

DEPARTMENT OF DEFENSE CONTRACTORS (Continued)

McDonnell Douglas Corp
ATTN: R. Halprin

Merritt CASES, Inc
ATTN: J. Merritt
ATTN: Library

Nathan M. Newmark Consult Eng Svcs
University of Illinois
ATTN: N. Newmark

Physics International Co
ATTN: J. Thomsen
ATTN: Technical Library
ATTN: L. Behrmann
ATTN: E. Moore
ATTN: F. Sauer

R & D Associates
ATTN: Tech Information Center
ATTN: J. Lewis
ATTN: W. Wright, Jr
ATTN: J. Carpenter
ATTN: R. Port
ATTN: P. Haas

Pacific-Sierra Research Corp
ATTN: H. Brode

Science Applications, Inc
ATTN: Technical Library

Science Applications, Inc
ATTN: D. Maxwell
ATTN: D. Bernstein

Science Applications, Inc
ATTN: W. Layson

Southwest Research Institute
ATTN: A. Wenzel
ATTN: W. Baker

SRI International
ATTN: B. Gasten
ATTN: Y. Gupta
ATTN: D. Keough
ATTN: G. Abrahamson

Systems, Science & Software, Inc
ATTN: T. Riney
ATTN: D. Grine
ATTN: Library
ATTN: T. Cherry

Systems, Science & Software, Inc
ATTN: J. Murphy

Terra Tek, Inc
ATTN: Library
ATTN: S. Green
ATTN: A. Abou-Sayed

Tetra Tech, Inc
ATTN: L. Hwang
ATTN: Library

Universal Analytics, Inc
ATTN: E. Field

DEPARTMENT OF DEFENSE CONTRACTORS (Continued)

TRW Defense & Space Sys Group
ATTN: P. Bhutta
ATTN: Technical Information Center
2 cy ATTN: N. Lipner

TRW Defense & Space Sys Group
ATTN: E. Wong
ATTN: P. Dai

AVCO Research & Systems Group
ATTN: Library A830

Boeing Company
ATTN: Aerospace Library

DEPARTMENT OF DEFENSE CONTRACTORS (Continued)

Weidlinger Assoc, Consulting Engineers
ATTN: M. Baron

Weidlinger Assoc, Consulting Engineers
ATTN: J. Isenberg

Westinghouse Electric Corp
Marine Division
ATTN: W. Volz